SPE 4316
Aug. 1974 JPT

Two-Phase Vertical Flow in Oil Wells—Prediction of Pressure Drop

G. L. Chierici, SPE-AIME, AGIP Exploration & Production
G. M. Ciucci, SPE-AIME, AGIP Exploration & Production
G. Sclocchi, AGIP Exploration & Production

Introduction

The polyphasic flow of Newtonian fluids in vertical pipes has been investigated both theoretically and experimentally by several authors.[1-18] Poettmann and Carpenter,[5] Ros,[11] Duns and Ros,[15] and Hagedorn and Brown[16] dealt with the problem of predicting pressure gradients in oil wells, where the flowing fluid may be a gas-oil-water mixture with interphase mass transfer.

Several applications and improvements of the equations proposed by the above authors have been published[20, 23-27]; empirical relationships have also been presented.[19, 21, 22]

A method for predicting two-phase pressure drop in vertical pipes was proposed by Orkiszewski.[17] This method, which has been widely accepted in the oil industry,[18, 28-31] is basically a combination of methods previously proposed by other authors,[2, 10, 15, 26] with some modifications as far as slug flow is concerned.

The same basic approach as Orkiszewski's has been adopted in the present work. Theoretical studies as well as experimental results presented in the technical literature have been examined and a set of equations has been selected that has proved to be particularly efficient in predicting pressure gradients in two-phase vertical flow. A new relationship has been developed to deal with the slug-froth flow regime.

Pressure Gradient and Flow Regimes

Starting from the macroscopic mechanical energy balance equation, the elementary pressure drop, dp, in a vertical pipe can be expressed as follows.

$$9.81 \times 10^5\, dp = \bar{\rho}\, g\, dD + \tau_f\, dD - \rho v dv \quad . \quad (1)$$

By making some approximations in evaluating the acceleration gradient, $\rho\, v\, dv$, which is almost always negligible, we have[17]

$$dp = \frac{\bar{\rho}\, g + \tau_f}{9.81 \times 10^5 - \frac{w_t\, q_g}{p\, A^2}}\, dD \quad . \quad . \quad . \quad . \quad (2)$$

Before integrating Eq. 2 numerically, the locally prevailing flow regime must be determined because the way both $\bar{\rho}$ and τ_f are to be evaluated depends on the flow regime.

The various ways a gas-liquid mixture can flow in a vertical pipe are usually grouped into three main flow regimes[10, 15]; that is, bubble-plug flow, slug-froth flow, and mist flow. A transition zone exists between the last two regimes.

By combining the experimental results by Griffith and Wallis[10] with those by Duns and Ros,[15] the following criteria have been proposed by Orkiszewski[17] for determining the flow regime.

Bubble-Plug Flow

$$(q_g/q_t) < N_v \quad . \quad . \quad . \quad . \quad . \quad . \quad . \quad . \quad . \quad . \quad . \quad (3)$$

Slug-Froth Flow

$$(q_g/q_t) > N_v\,, \quad . \quad . \quad . \quad . \quad . \quad . \quad . \quad . \quad . \quad . \quad (4a)$$

A combination of mass-transfer flow regime methods is presented for predicting two-phase pressure gradients in oil wells with low to medium GOR's. New relationships are proposed for the slug-froth flow regime to improve the accuracy of the calculated local thermodynamic parameters.

and

$$N_{gv} < (50 + 36\,N_{lv}) \quad (4b)$$

Transition Flow

$$(50 + 36\,N_{lv}) \leq N_{gv} \leq (75 + 84\,N_{lv}^{0.75}) \quad (5)$$

Mist Flow

$$N_{gv} > (75 + 84\,N_{lv}^{0.75}), \quad (6)$$

where

$$N_v = 1.071 - 7.35\,\frac{v_m^2}{g\,d_h}, \quad (7a)$$

with the limit $N_v \geq 0.18$, (7b)

$$N_{gv} = v_{sg}\sqrt[4]{\frac{\rho_l}{g\,\sigma}}, \quad (7c)$$

$$N_{lv} = v_{sl}\sqrt[4]{\frac{\rho_l}{g\,\sigma}} \quad (7d)$$

The regions of existence of the various flow regimes are shown in Fig. 1. Note that the boundary between bubble- and slug-flow regimes, expressed by Eqs. 3 and 7a, results in a family of curves (Fig. 1), each corresponding to a different set of ρ_l, σ, and d_h.

Average Density of the Flowing Fluid

Determining the average density, $\bar{\rho}$, of a gas-liquid mixture,

$$\bar{\rho} = \rho_g H_g + \rho_l (1 - H_g), \quad (8)$$

relies upon determining the volume fraction H_g occupied by the gas phase. The way H_g is calculated depends on the flow regime, as explained in the following.

Bubble-Plug Flow

Theoretical studies[1,3] as well as experimental results[7-10,12-14] have ascertained that in the bubble-plug flow regime the gas phase flows upward with a velocity higher than the liquid phase, their difference being termed gas slip velocity, v_s. Therefore, by definition,

$$v_s = \frac{v_{sg}}{H_g} - \frac{v_m - v_{sg}}{1 - H_g}; \quad (9)$$

hence,

$$H_g = 0.5\left\{\left(1 + \frac{v_m}{v_s}\right) - \left[\left(1 + \frac{v_m}{v_s}\right)^2 - 4\,\frac{v_{sg}}{v_s}\right]^{1/2}\right\}. \quad (10)$$

Correlations for calculating v_s have been presented by several authors.[32,33] In the present work, a constant value $v_s = 24$ cm/sec, as proposed by Griffith and Wallis,[10] has been adopted.

Slug-Froth Flow

In this regime the liquid in the liquid slugs occupies the whole section of the pipe. As a consequence, the liquid velocity in the central part of a slug (that is, far enough from slug ends not to be affected by end effects) is equal to the total volumetric velocity, v_m. The difference, $v_g - v_m$, between the velocity of the gas bubble and that of the liquid in the central part of the slug is termed the relative bubble-rise velocity, v_b.

By definition,

$$v_b = \frac{v_{sg}}{H_g} - v_m; \quad (11)$$

hence,

$$H_g = \frac{v_{sg}}{v_m + v_b} = \frac{q_g}{q_t + A v_b}. \quad (12)$$

According to Griffith and Wallis,[10] the following relationship holds:

$$v_b = C_1\,C_2\sqrt{g\,d_h}, \quad (13)$$

where C_1 is a function of $(N_{Re})_b$ (see Fig. 8 of Ref. 10) and C_2 is a function of both $(N_{Re})_b$ and $(N_{Re})_t$.

Griffith and Wallis experimentally determined the C_2 function for $(N_{Re})_t$ values between zero and 6,000. Their results are reported in Fig. 9 of Ref. 10. Nicklin *et al.*[14] ran experimental determinations of v_b also in the field $(N_{Re})_t > 6{,}000$; on the basis of the results obtained, they proposed the following equation:

$$v_b = \Lambda\,v_m + 0.35\sqrt{g\,d_h}, \quad (14)$$

where

$$\Lambda = 0.2 = \text{constant when } (N_{Re})_t > 6{,}000.$$

For $(N_{Re})_b > 0.4$, and therefore[10] $C_1 = 0.35$, from Eqs. 13 and 14 it can be derived that

$$C_2 = \frac{1}{1 - \Lambda\,\frac{(N_{Re})_t}{(N_{Re})_b}}. \quad (15)$$

In Fig. 2, Λ values computed according to Eq. 15 from the experimental data by Griffith and Wallis (Table 3 of Ref. 10) are reported together with Λ values presented by Nicklin *et al.* (Fig. 6 of Ref. 14). A very good match between the two sets of Λ values is observed. Therefore, Eq. 15 with $\Lambda = 0.2 =$ constant can be used to extrapolate in the $(N_{Re})_t > 6{,}000$ field the C_2 curves presented by Griffith and Wallis.[10]

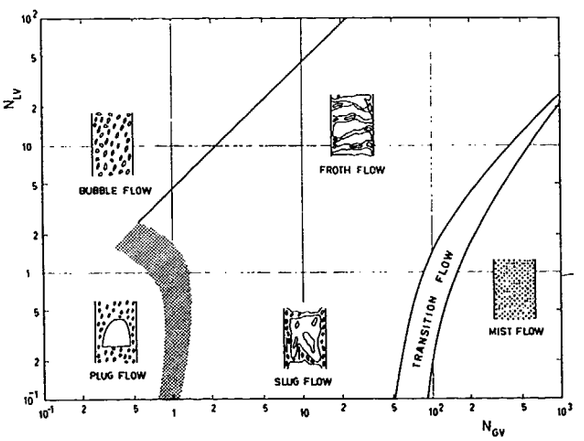

Fig. 1—Flow regime map, as from Eqs. 3 through 6.

The C_2 curves extrapolated according to Eq. 15 are compared in Fig. 3 with the C_2 curves calculated according to Orkiszewski[17] (Eqs. C-7 through C-9). (Orkiszewski Eq. C-9 is affected by a printing error. A pair of parentheses has been omitted.)

Fig. 3 shows that Orkiszewski extrapolation equations are not in agreement with Nicklin *et al.*[14] experimental results. Moreover, at the connection point between Griffith and Wallis curves and Orkiszewski extrapolated curves, a discontinuity occurs in the C_2 function and in its derivative.

Mist Flow

Experimental work by Duns and Ros[15] has ascertained that virtually no slip occurs between the gas phase and the entrained liquid droplets in mist regime. Therefore,

$$H_g = \frac{q_g}{q_t} \quad . \quad . \quad . \quad . \quad . \quad . \quad . \quad . \quad . \quad . \quad . \quad (16)$$

Friction-Loss Gradient

The friction loss gradient, τ_f, is calculated according to the classical equation

$$\tau_f = f \rho \frac{v^2}{2 d_h} \quad , \quad . \quad . \quad . \quad . \quad . \quad . \quad . \quad . \quad . \quad . \quad (17)$$

where the friction factor, f, is obtained by entering the Moody[2] diagram (Fig. 4) with the appropriate N_{Re} and ξ/d_h values. What density, velocity, and Reynolds number are to be used depends on the flow regime, as explained in the following.

Bubble-Plug Flow

As the gas bubbles are dispersed inside the liquid, they do not affect friction losses at the pipe wall. The density and velocity values to be entered in Eq. 17 are therefore ρ_l and v_l; f is evaluated from $(N_{Re})_l$.

Slug-Froth Flow

As previously explained, the liquid velocity in the central part of a slug is v_m. Assuming that only the liquid slugs contribute to the friction losses, we have

$$\tau_f = (1 - H_g) f \rho_l \frac{v_m^2}{2 d_h} \quad , \quad . \quad . \quad . \quad . \quad . \quad (18)$$

where f is evaluated according to $(N_{Re})_l$. The $(1 - H_g)$ factor represents the fractional length of the pipe occupied by the liquid slugs.

Aziz *et al.*[18] have recently proposed an equation identical with Eq. 18.

Mist Flow. According to Duns and Ros,[15] the friction losses in the mist flow regime are due to the gas phase only. Therefore, ρ_g and v_{sg} values must be used in Eq. 17.

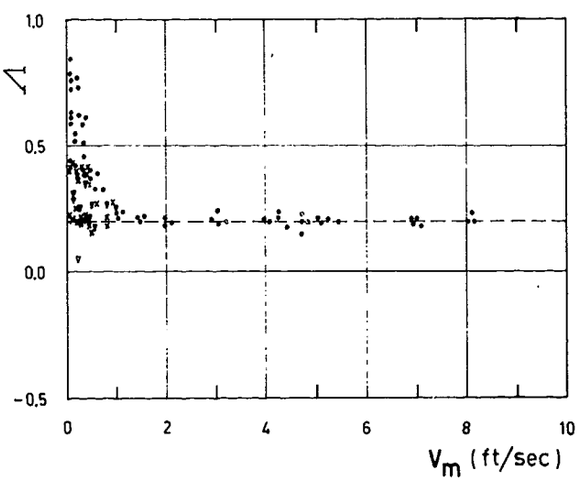

Fig. 2—Comparison between Lambda values calculated from Ref. 10 experimental data (crosses: d_h = 3/4 in.; triangles: d_h = 1 in.) and Lambda values reported in Ref. 14 (dots).

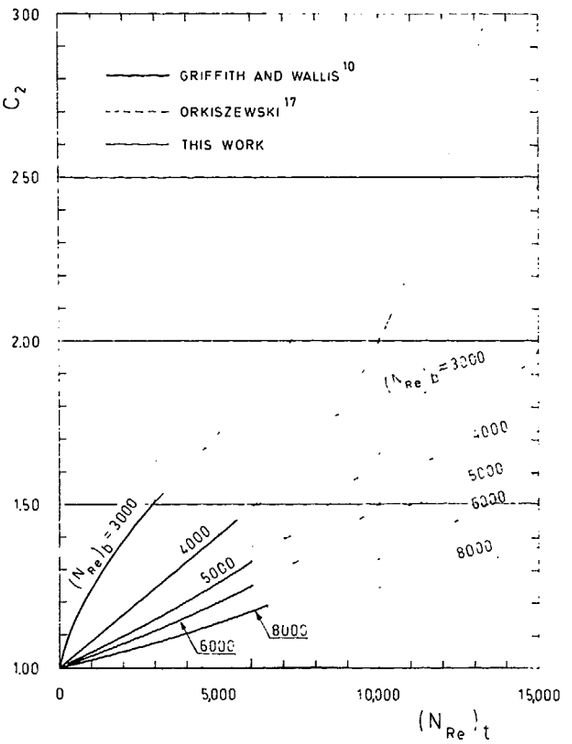

Fig. 3—Comparison between C_2 values extrapolated according to Eq. 15 (assuming $\Lambda = 0.2$) and C_2 values calculated according to Orkiszewski[17] equations.

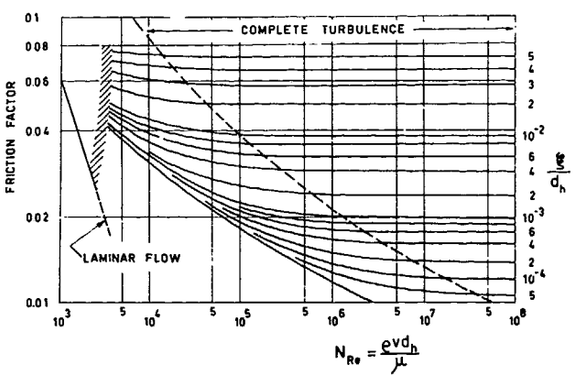

Fig. 4—Moody[2] diagram.

The liquid phase indirectly contributes to friction losses through the formation of a "wavy" film, adhering to the pipe wall, that increases the roughness of the pipe wall. The friction factor, f, must be evaluated according to $(N_{Re})_g$ and to the liquid film "roughness," ξ.

The roughness of the liquid film is due to the drag exerted by the flowing gas and is opposed by the liquid surface tension. According to Duns and Ros,[15] the Weber number resulting from the film "roughness" and the gas parameters is a function of the dimensionless group $(N_\mu N_{We})$; namely,

$$\left.\begin{aligned} &N_{We} = 34; \\ &\text{that is,} \\ &\xi = 34\,\frac{\sigma}{\rho_g v^2_{sg}} \end{aligned}\right\} \quad \ldots\ldots\ldots \quad (19)$$

when $(N_\mu N_{We}) \leq 4.5 \times 10^{-3}$.

And

$$\left.\begin{aligned} &N_{We} = 157.4\,(N_\mu N_{We})^{0.28}; \\ &\text{that is,} \\ &\xi = \frac{157.4}{\sigma}\left(\frac{\mu_l^2}{\rho_l}\right)^{0.28}\left(\frac{\sigma^2}{\rho_g v^2_{sg}}\right)^{0.72} \end{aligned}\right\} \quad \ldots \quad (20)$$

when $(N_\mu N_{We}) > 4.5 \times 10^{-3}$.

Should the ξ value, as obtained from the above equations, be less than the original pipe roughness, the value of the original pipe roughness is adopted in the calculations.

When $(\xi/d_h) > 0.05$, the flow string restrictions due to the liquid film roughness must be accounted for. Therefore,

$$v_{sg} = \frac{q_g}{A\left(1 - 2\frac{\xi}{d_h}\right)^2} \quad \ldots\ldots \quad (21)$$

As $(\xi/d_h) = 0.05$ is the maximum relative roughness value reported in the Moody diagram, for $(\xi/d_h) > 0.05$, the f value is computed according to the following empirical relationship, which is valid in completely turbulent flow conditions only:

$$f = \frac{1}{4\left[\log\left(0.27\frac{\xi}{d_h}\right)\right]^2} + 0.268\left(\frac{\xi}{d_h}\right)^{1.73} \quad \ldots\ldots\ldots \quad (22)$$

Average Density and Friction Gradient in Transition Flow

Linear interpolation as proposed by Duns and Ros[15] is the only method that has been published for calculating $\bar{\rho}$ and τ_f in the transition flow regime. This method is outlined below.

1. From the local value of N_{lv}, the value of N_{gv} corresponding to the boundary between slug and transition flow regimes (Eq. 4b) is calculated; hence,

$$(q_g)_S = (N_{gv})_S\, A \sqrt[4]{\frac{g\,\sigma}{\rho_l}} \quad \ldots\ldots \quad (23)$$

The fluid average density $(\bar{\rho})_S$ and friction-loss gradient $(\tau_f)_S$ at the boundary between the slug and transition flow regimes are then calculated using the equations for the slug-froth flow regime and assuming $(q_g)_S$ as fictitious gas flow rate.

2. From the local value of N_{lv}, the value of N_{gv} corresponding to the boundary between transition and mist flow regimes (Eq. 6) is calculated; hence,

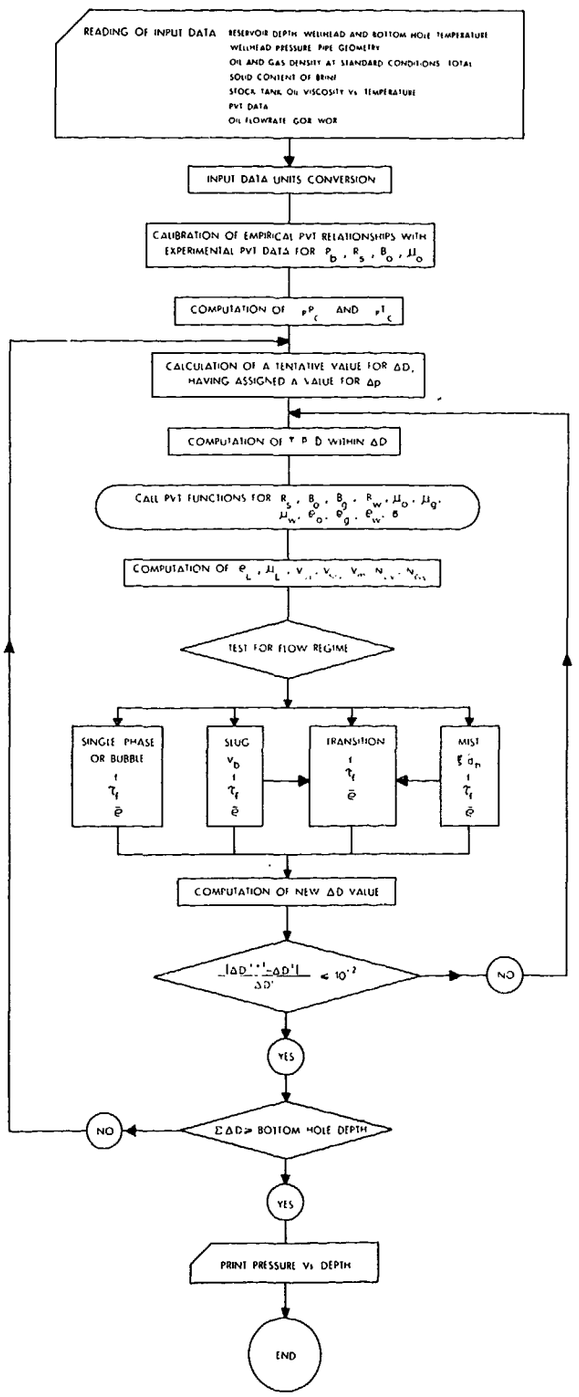

Fig. 5—Flow chart of the computer program.

$$(q_g)_M = (N_{gv})_M A \sqrt[4]{\frac{g\sigma}{\rho_l}} \quad . \quad . \quad . \quad . \quad . \quad . \quad . \quad (24)$$

To keep the gas mass flow rate constant, a modified value $(\rho_g)_M$ of the gas density is calculated as

$$(\rho_g)_M = \rho_g \frac{q_g}{(q_g)_M} \quad . \quad . \quad . \quad . \quad . \quad . \quad . \quad . \quad (25)$$

The fluid average density $(\bar{\rho})_M$, and friction-loss gradient, $(\tau_f)_M$, at the boundary between the transition and mist flow regimes are then computed with the equations for the mist flow regime, using $(q_g)_M$ and $(\rho_g)_M$ as fictitious gas flow rate and gas density.

3. To calculate $\bar{\rho}$, linear interpolation between $(\bar{\rho})_S$ and $(\bar{\rho})_M$ is employed as follows

$$\bar{\rho} = (\bar{\rho})_S \frac{(N_{gv})_M - N_{gv}}{(N_{gv})_M - (N_{gv})_S} + (\bar{\rho})_M \frac{N_{gv} - (N_{gv})_S}{(N_{gv})_M - (N_{gv})_S} \quad . \quad . \quad . \quad . \quad (26)$$

A similar equation is used for interpolating τ_f from $(\tau_f)_S$ and $(\tau_f)_M$ values.

Comments on the Computation Technique

The flow chart of the computer program used in this work is presented in Fig. 5.

In the course of the work it has been found that pressure gradient values are very sensitive to the values attributed to thermodynamic parameters of flowing fluids. Since experimental PVT data are seldom available for temperatures other than reservoir temperature and for pressures outside the range of reservoir pressures, recourse to empirical correlations cannot be avoided. Whenever possible, care has been taken to calibrate the chosen correlations with PVT data measured at reservoir conditions.

Local values of fluid characteristics have been derived from standard correlations as concerns gas compressibility,[34-36] gas viscosity,[37] water formation volume factor,[38] water viscosity,[39] and gas/oil interfacial tension.[40]

As concerns oil PVT parameters, the following relationships[41-44] have been used:

$$p = C\left(\frac{R_s}{\gamma_g}\right)^{0.83} \frac{10^{(0.00164\,T - 0.419)}}{10^{0.0125\,(°\mathrm{API})}} \quad . \quad . \quad (27a)$$

for API gravities lower than 15°;

$$p = C\frac{T}{\gamma_g}[0.0859\,(10^{1.21\gamma}) - 0.0766] \quad . \quad . \quad . \quad . \quad . \quad . \quad . \quad . \quad . \quad . \quad . \quad (27b)$$

for API gravities higher than 15°C; and

$$B_o = C + 3.81 \times 10^{-4}\left[2.5\,R_s\left(\frac{\gamma_g}{\rho_{o,sc}}\right)^{0.5} + T - 255.6\right]^{1.175} \quad . \quad . \quad . \quad . \quad . \quad (27c)$$

It has been assumed that oil and gas are locally in equilibrium. Local pressure is therefore equal to the bubble-point pressure of the oil phase.

The production GOR is obviously a limiting value for R_s. When the R_s value obtained from Eqs. 27a or 27b is greater than the well GOR, the latter is adopted for R_s and the corresponding local bubble-point pressure is calculated.

The values of the C constants appearing in Eqs. 27 are calculated by entering the corresponding equation with the experimental values pertaining to reservoir oil at reservoir temperature and bubble-point pressure.

Oil viscosity is calculated according to Chew and Connally.[45] The stock-tank oil viscosity at T is either interpolated using the ASTM D341-43 procedure or obtained from empirical correlations.[46,47]

The experimental value of the oil viscosity at reservoir temperature and bubble-point pressure is compared with the corresponding value obtained by the above method, and the two values are made to coincide by shifting the curve for the stock-tank oil viscosity vs temperature.

When the oil is locally undersaturated, both $B_{o,b}$ and $\mu_{o,b}$ values are corrected accordingly.[47,48]

When water is present in the flowing fluid, the following empirical relationships are used for the liquid phase:

$$\rho_l = \frac{1}{q_l}\left[\left(\rho_{o,sc} + \rho_{g,sc}R_s\right)q_{o,sc} + \rho_{w,sc}\,q_{w,sc}\right] \quad . \quad . \quad . \quad . \quad . \quad . \quad . \quad . \quad . \quad . \quad . \quad (28a)$$

$$\mu_l = \frac{1}{q_l}(q_{o,sc}\,B_o\,\mu_o + q_{w,sc}\,B_w\,\mu_w) \quad . \quad . \quad (28b)$$

ρ_l and μ_l values calculated according to Eq. 28 are sufficiently accurate at low water cuts only, as they do not account for emulsification and slippage between oil and water.

Predicted and Actual Pressure Drops—Analysis of Some Well Cases

To test its validity, the method outlined has been applied to 31 oil wells and to 6 gas wells where pressure drops were known from pressure surveys. The results obtained are analyzed below.

Oil Wells

Well flow conditions and fluid characteristics for the 31 oil wells considered are presented in Table 1.

A small water production was present in eight wells. Their water cuts were nevertheless too low for inferring any conclusion about the validity of the method to deal with three-phase flow.

Below is the range of parameters involved in this investigation of pressure-drop calculations.

Oil Characteristics	
API gravity	8.3° through 46°
Bubble-point pressure at reservoir temperature (p_b), kg/sq cm abs	56 through 405
Solution GOR (R_s) of saturated reservoir oil, scm per cu m of stock-tank oil	22.9 through 401.6
Gravity (γ_g) of gas in solution	0.571 through 1.705 (air = 1)
Viscosity ($\mu_{o,b}$) of saturated reservoir oil, cp	0.16 through 77.2

TABLE 1—OIL WELLS—SUMMARY OF FLOW CONDITIONS AND FLUID CHARACTERISTICS FOR THE CASES CONSIDERED

	Well Flow Conditions								Characteristics of Produced Fluids					
							Temperature		Reservoir Oil at Bubble-Point Pressure					
Case	API Gravity of Crude (dimensionless)	GOR (scm/cu m)	Water Cut (%)	Oil Flow Rate (cu m/D)	Wellhead Pressure (kg/sq cm abs)	Tubing Diameter (nominal) (in.)	Wellhead (°C)	Bottom-hole (°C)	p_b (kg / sq cm abs)	R_s (scm/cu m)	B_o (dimensionless)	μ_o (cp)	Separator Gas Gravity (air = 1.00)	Total Dissolved Solids (gm/l)
1	8.3	25.9	0.3	83	15.7	5	47.5	107	56	25.9	1.1530	77.2	1.705	63
2	8.3	25.9	0.15	148	14.7	5	57	109	56	25.9	1.1530	77.2	1.705	63
3	9	22.9	0.2	7	7	5	20	90	68	22.9	1.1398	49.2	1.567	30
4	9	22.9	0.2	147	11.6	5	32	91	68	22.9	1.1398	49.2	1.567	30
5	11.8	29.9	0.5	23	15.5	5	27	88	124	29.9	1.1404	35.3	0.938	71
6	11.8	29.9	0.1	133	36.9	5	29	89	124	29.9	1.1404	35.3	0.938	71
7	12.5	37.5	0.1	121	40.1	5	40	106	157	37.5	1.1401	23.3	1.268	30
8	12.5	37.5	0.1	175	41.5	5	58	108	157	37.5	1.1401	23.3	1.268	30
9	16.7	90.8	0	830.3	42.6	5	59	87	171	90.8	1.2974	4.03	0.708	—
10	17.2	90.8	0	656.3	54.2	5	51.6	87	171	90.8	1.2974	4.03	0.708	—
11	19.2	90.8	0	609.6	57.3	2⅞	48.3	86	171	90.8	1.2974	4.03	0.708	—
12	19.2	90.8	0	672	39.6	2⅞	56	86.6	171	90.8	1.2974	4.03	0.708	—
13	19.2	90.8	0	1,092	30.2	2⅞	59.4	86.6	171	90.8	1.2974	4.03	0.708	—
14	25	68.0	0	40.6	8	2⅞	40	92.5	96	68.0	1.2601	2.07	0.571	—
15	25	68.0	0	56.2	8	2⅞	40	92.5	96	68.0	1.2601	2.07	0.571	—
16	31.3	163.1	0	85	111.6	3½	40	85	264	163.1	1.4437	0.73	0.920	—
17	31.3	159.8	0	422	93	3½	40	85	264	163.1	1.4437	0.73	0.920	—
18	32.2	152.1	0	416	110	2⅞	42	89	243	152.1	1.4626	0.67	0.920	—
19	32.8	132	0	350.4	63	2⅞	41	80	238	169.3	1.5161	0.49	0.701	—
20	32.8	134	0	573.6	69.5	2⅞	42	80	238	169.3	1.5161	0.49	0.701	—
21	32.8	138	0	648	69.5	2⅞	42	80	238	169.3	1.5161	0.49	0.701	—
22	40.3	167.8	0	30.5	96.5	2⅞	33.4	75	207	167.8	1.6050	0.35	0.750	—
23	40.3	167.8	0	52.6	94.5	2⅞	32	75	207	167.8	1.6050	0.35	0.750	—
24	40.3	167.8	0	76.4	92	2⅞	31.9	75	207	167.8	1.6050	0.35	0.750	—
25	40.3	167.8	0	179	82.5	2⅞	37	75	207	167.8	1.6050	0.35	0.750	—
26	42	315	0	198	241.2	*	82	147	405	315.0	2.0710	0.21	0.764	—
27	42	314	0	902	234.5	*	106	147	405	315.0	2.0710	0.21	0.764	—
28	42	269	0	936	194.9	*	102	147	405	315.0	2.0710	0.21	0.764	—
29	42	297	0	1,848	189.8	*	116	147	405	315.0	2.0710	0.21	0.764	—
30	46	404.6	0	34.3	154.2	2⅞	34	111.2	287	404.6	2.4360	0.16	0.710	—
31	46	404.6	0	69.9	158.6	2⅞	34	111.1	287	404.6	2.4360	0.16	0.710	—

*Flow is through the annulus between 7⅝-in. casing and 2⅞-in.tubing.

TABLE 2—OIL WELLS—SUMMARY OF RESULTS

Case No.	Bottom-hole Pressure, Flowing (kg/sq cm abs)	Pressure Drop Between Bottom-hole and Wellhead (kg/sq cm)		Percentage Error Between Calculated and Measured Δp	Depth of Producing Interval (meters)	Length of Flow String Where the Various Flow Regimes Prevail (meters)				
		Measured	Calculated			Single-phase	Bubble or Plug	Slug or Froth	Transition	Mist
1	334.6	318.9	304.5	− 4.5	3,300	2,953	330	17	0	0
2	334.9	320.2	303.3	− 5.3	3,300	2,925	269	106	0	0
3	292.8	285.8	298.5	+ 4.4	3,200	2,655	545	0	0	0
4	314.5	302.9	294.4	− 2.8	3,200	2,662	362	172	0	0
5	321.1	305.6	278.3	− 8.9	3,100	2,137	963	0	0	0
6	314.7	277.8	278.4	+ 0.22	3,100	2,350	750	0	0	0
7	317.9	277.8	280.3	+ 0.90	3,100	2,005	1,095	0	0	0
8	320.2	278.7	277.3	− 0.50	3,100	1,945	1,155	0	0	0
9	215.3	172.7	173	+ 0.17	2,331	669	526	1,136	0	0
10	234	179.8	180	+ 0.11	2,331	809	531	991	0	0
11	242.2	184.9	191	+ 3.3	2,310	1,010	482	818	0	0
12	231.6	192	188	− 2.1	2,310	748	485	1,077	0	0
13	228.5	198.3	220	+10.9	2,310	836	438	1,036	0	0
14	194.2	186.2	190.1	+ 2.1	2,670	1,488	804	378	0	0
15	197.2	189.2	188.6	− 0.32	2,670	1,467	591	612	0	0
16	270.7	159.1	166.3	+ 4.5	2,331	227	2,104	0	0	0
17	250	157	164	+ 4.4	2,331	0	524	1,807	0	0
18	278.1	168.1	166	− 1.2	2,331	532	571	1,228	0	0
19	209	146	130.6	−10.5	2,150	0	0	2,150	0	0
20	222.5	153	140	− 8.5	2,150	0	166	1,984	0	0
21	226.5	157	143.8	− 8.4	2,150	0	215	1,935	0	0
22	251.3	154.8	163	+ 5.3	2,450	774	1,676	0	0	0
23	246.7	152.2	158.4	+ 4.1	2,450	776	1,674	0	0	0
24	241.6	149.6	158.8	+ 6.1	2,450	828	527	1,095	0	0
25	226.9	144.4	155.5	+ 7.7	2,450	667	525	1,258	0	0
26	464.9	223.7	223.8	0.0	4,000	1,403	2,597	0	0	0
27	444.6	210.1	222	+ 5.7	4,000	1,406	628	1,966	0	0
28	399.2	204.3	220	+ 7.7	4,000	0	1,034	2,966	0	0
29	402.8	213	217	+ 1.9	4,000	0	1,302	2,698	0	0
30	326.3	172.1	158	− 8.2	3,210	814	2,396	0	0	0
31	326.2	167.6	160	− 4.5	3,210	749	996	1,465	0	0

Flow Conditions	
Oil flow rate ($q_{o,sc}$) cu m/D, stock-tank oil	7 through 1,848
GOR (R), scm per cu m of stock-tank oil	22.9 through 404.6
Tubing diameter, nominal, in.	2⅞ through 5
Depth of producing interval, m	2,150 through 4,000
Tubing pressure, flowing (p_{tf}), kg/sq cm abs	7 through 241.2
Bottom-hole pressure, flowing (p_{wf}), kg/sq cm abs	194.2 through 464.9
$\Delta p = p_{wf} - p_{tf}$, kg/sq cm	144.4 through 320.2
Wellhead temperature, °C	20° through 116°
Bottom-hole temperature, °C	75° through 147°

The results obtained are compared with measured pressure drops in Table 2 and in Fig. 6. Deviations between predicted and measured pressure drops are

Average error, percent	+ 0.12
Average absolute error, percent	4.36
Extreme limits of error, percent	
Case 13	+ 10.9
Case 19	− 10.5
Standard deviation, percent	5.42

A fairly good agreement has also been found between computed and measured pressure traverses, when the latter were available. Three examples are shown in Fig. 7.

The maximum lengths of well string where the same flow regime was found to prevail were (Table 2),

Single-phase liquid flow (Case 1), m	2,953
Bubble and plug flow (Case 26), m	2,597
Plug and froth flow (Case 28), m	2,966

Neither transition nor mist flow regimes occurred in the cases considered; therefore, it was not possible to test the related pressure-drop correlation methods.

From Table 3, where all cases ... been grouped according to the range of API gravity, GOR, oil flow rate, and oil viscosity, it is apparent that the accuracy of the results is not affected by the range of the above parameters.

Gas Wells

Six cases of gas wells producing free water have been considered. Gas/water ratios (GWR's) ranged between 8,470 and 55,500 scm/cu m. Other well parameters are reported in Table 4.

According to the criteria described previously, a slug-froth flow regime should prevail in all six gas wells. Pressure drops computed according to such a flow regime were much greater than the measured pressure drops.

Intuitively, it seems unlikely that a slug-froth flow regime can prevail at GWR's as high as the ones existing in the wells considered. A mist flow regime appears to be more realistic.

On the other hand, according to the criteria proposed by Ros[11] and by Duns and Ros,[15], mist flow can prevail only for $N_{gv} > 75$ (Fig. 1 and Eq. 6). For the case of a 3½-in. tubing and 80 kg/sq cm wellhead pressure, this corresponds to $q_{g,sc} > 500{,}000$ scm/D. Therefore, the use of Duns and Ros correlations results in the unrealistic conclusion that, *independent of gas/liquid value*, mist flow regime cannot prevail unless very high gas flow rates are established.

To overcome this impasse, no consideration was given to local N_{gv} and N_{lv} values and the computer program was forced to evaluate the pressure gradients according to mist flow regime. For gas wells, the resulting calculation method is practically equivalent to the one proposed by Cullender and Smith,[6] when Cullender and Smith's is corrected for the presence of free water in the well effluent. The only difference is that $\bar{\rho}$ value, instead of ρ_g value, is used by Cullender and Smith[6] to evaluate τ_f.

Pressure drops predicted according to the above-outlined method are compared (in Table 4) with measured values. From the same table the following deviation values are derived.

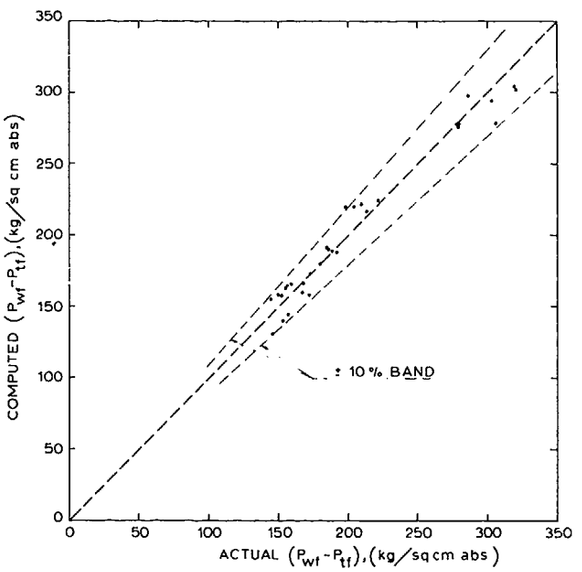

Fig. 6—Computed pressure drops ($p_{wf} - p_{tf}$) vs measured pressure drops.

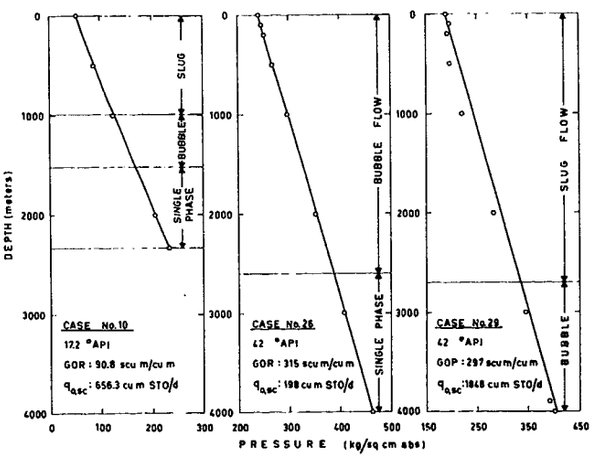

Fig. 7—Calculated pressure traverses compared with measured pressure values (dots) for three typical oilwell cases.

Average error, percent	− 10.5
Average absolute error, percent	18.8
Standard deviation, percent	23.5

It is apparent that for gas wells producing at high GWR's the predicted pressure drops are much less accurate than for oil wells producing at low to medium GOR's.

Conclusions

1. A method has been presented for predicting pressure drops in two-phase vertical flow with mass transfer between the flowing phases.

The average density of the flowing fluid and the friction losses are calculated according to the locally prevailing flow regime. Griffith and Wallis[10] and Duns and Ros[15] correlations are used to evaluate the regions of existence of the various flow regimes.

2. A new relationship has been proposed for extrapolating at $(N_{Re})_b > 6{,}000$ and $(N_{Re})_t > 6{,}000$ the Griffith and Wallis[10] correlation used to calculate the average fluid density in the slug-froth flow regime. The method is based on a combined interpretation of Griffith and Wallis and Nicklin *et al*,[14] experimental data. The proposed relationship does not contain empirical correction coefficients (Orkiszewski[17] liquid distribution coefficient Γ) whose physical meaning is somewhat obscure.

3. Methods have been presented for improving the accuracy of the empirical relationships used to evaluate oil formation volume factor, B_o, oil viscosity, μ_o, and gas solubility in oil, R_s, as functions of temperature and pressure, through calibration against experimental PVT data.

Calibration of fluid characteristics against PVT data is of the utmost importance for the reliability of

TABLE 3—OIL WELLS—ANALYSIS OF RESULTS

Range of Values	Number of Cases Examined	Average Deviation (percent)	Average Absolute Deviation (percent)	Standard Deviation (percent)
1a—API Gravity Lower Than 20°				
$q_{o,sc} < 150$ cu m/D	7	−2.28	3.86	4.71
$q_{o,sc} > 150$ cu m/D	6	+1.98	2.85	4.73
Over-all Values	13	−0.32	3.39	4.72
1b—API Gravity Between 20° and 35°				
$q_{o,sc} < 150$ cu m/D	3	+2.09	2.31	2.87
$q_{o,sc} > 150$ cu m/D	5	−4.84	6.60	7.40
Over-all Values	8	−2.24	4.99	6.11
1c—API Gravity Higher Than 35°				
$q_{o,sc} < 150$ cu m/D	5	+0.56	5.64	5.82
$q_{o,sc} > 150$ cu m/D	5	+4.60	4.60	5.56
Over-all Values	10	+2.58	5.12	5.69
2a—*R* Lower Than 150 scm/cu m				
$q_{o,sc} < 150$ cu m/D	9	−1.68	3.27	4.22
$q_{o,sc} > 150$ cu m/D	9	−1.72	4.94	6.56
Over-all Values	18	−1.70	4.11	5.52
2b—*R* Higher Than 150 scm/cu m				
$q_{o,sc} < 150$ cu m/D	6	+1.22	5.45	5.63
$q_{o,sc} > 150$ cu m/D	7	+3.74	4.09	5.01
Over-all Values	13	+2.58	4.72	5.31
3a—Oil Flow Rate Lower Than 150 cu m/D				
API gravity lower than 35°	10	−0.97	3.39	4.25
API gravity higher than 35°	5	+0.56	5.64	5.82
Over-all Values	15	−0.46	4.14	4.83
3b—Oil Flow Rate Higher Than 150 cu m/D				
API gravity lower than 35°	11	−1.12	4.55	6.09
API gravity higher than 35°	5	+4.60	4.60	5.56
Over-all Values	16	+0.67	4.57	5.93
4a—Reservoir Oil μ at Bubble Point Lower Than 2 cp				
$q_{o,sc} < 150$ cu m/D	6	+1.22	5.45	5.63
$q_{o,sc} > 150$ cu m/D	10	−0.12	5.60	6.55
Over-all Values	16	+0.38	5.54	6.22
4b—Reservoir Oil μ at Bubble Point Higher Than 2 cp				
$q_{o,sc} < 150$ cu m/D	9	−1.58	3.27	4.22
$q_{o,sc} > 150$ cu m/D	6	+1.98	2.85	4.73
Over-all Values	15	−0.15	3.10	4.43

calculated pressure drops. Any effort in improving pressure-drop prediction methods has little meaning if accurate data for thermodynamic parameters of flowing fluids are not available.

4. The proposed method has been tested for validity on 31 actual oilwell cases covering a broad range of API gravity, GOR, oil flow rate, and pressure drop (Tables 1 and 2). The validity of the method is shown by the following results, referring to the deviation between predicted and actual pressure drops.

Average error, percent	+ 0.12
Average absolute error, percent	4.36
Standard deviation, percent	5.42

It is shown that the accuracy of the method does not depend on API gravity, GOR, and oil flow rate ranges, at least for the limits within which the above parameters have been investigated (Table 3).

5. The method has also been tested on six cases of gas wells producing small amounts of free water. The results obtained show that the accuracy of the proposed method becomes poor at very high gas-liquid ratios.

Nomenclature

A = flow area of pipe, sq cm
B = formation volume factor (volume at local pressure and temperature divided by volume at standard conditions), dimensionless
C_1 = function of $(N_{Re})_b$, Eq. 13, dimensionless
C_2 = function of $(N_{Re})_b$ and $(N_{Re})_t$, Eqs. 13 and 15, dimensionless
d_h = pipe hydraulic diameter (= $4A$/wetted perimeter), cm; for round pipe, $d_h = 2r$; for annulus, $d_h = 2(r_e - r_i)$
D = depth, cm
f = Moody friction factor, Fig. 4, dimensionless
g = acceleration of gravity, cm/sq sec
H_g = flowing gas fraction, dimensionless
N_{gv} = dimensionless gas velocity, Eq. 7c
N_{lv} = dimensionless liquid velocity, Eq. 7d
N_v = over-all dimensionless velocity, Eqs. 7a and 7b

N_{We} = Weber number = $\rho_g \frac{v_{Sg}^2 \xi}{\sigma}$, dimensionless

N_μ = viscosity number = $\frac{\mu_l^2}{\rho_l \sigma \xi}$, dimensionless

$(N_{Re})_b$ = bubble Reynolds number = $100 \frac{\rho_l v_b d_h}{\mu_l}$, dimensionless

$(N_{Re})_g$ = gas Reynolds number = $100 \frac{\rho_g V_{Sg} d_h}{\mu_g}$, dimensionless

$(N_{Re})_l$ = liquid Reynolds number = $100 \frac{\rho_l v_l d_h}{\mu_l}$, dimensionless

$(N_{Re})_t$ = over-all Reynolds number = $100 \frac{\rho_l v_m d_h}{\mu_l}$, dimensionless

p = pressure, kg/sq cm abs
q = volumetric flow rate at local pressure and temperature, cc/sec
q_t = total fluid flow rate = $q_g + q_o + q_w$, cc/sec
r = radius, cm
R = gas-oil ratio, scm/cu m of stock-tank oil
R_s = gas solubility in oil, scm/cu m of stock-tank oil
T = temperature, °K
v = velocity, cm/sec
v_b = relative bubble-rise velocity = $v_g - v_m$, cm/sec
v_g = gas velocity = $q_g/H_g A$, cm/sec
v_l = liquid velocity = $q_l/[(1 - H_g) A]$ cm/sec
v_m = over-all superficial velocity = $(q_g + q_l)/A$, cm/sec
v_s = gas slip velocity = $v_g - v_l$, cm/sec
v_{Sg} = superficial velocity of gas = q_g/A, cm/sec
v_{Sl} = superficial velocity of liquid = q_l/A, cm/sec
w_t = total mass flow rate, gm/sec
y = mol fraction of gas dissolved in the oil, dimensionless
γ_g = gas specific gravity (air = 1)
Λ = dimensionless coefficient, Eqs. 14 and 15
μ = in-situ viscosity, cp
ξ = pipe wall roughness, cm
ρ = in-situ density, gm/cc
$\bar{\rho}$ = in-situ density of the flowing fluid, gm/cc
σ = interfacial tension between the gaseous and liquid phases, dyne/cm
τ_f = friction loss gradient, dyne/sq cm × cm

TABLE 4—GAS WELLS—BASIC DATA AND RESULTS OBTAINED

Case	Gas-Water Ratio (scm/cu m)	Gas Flow Rate (scm/D)	Gas Gravity (air = 1.0)	Total Solids Content of Produced Brine (gm/l)	Tubing Diameter (nominal) (in.)	Depth of Producing Interval (meters)	Wellhead Conditions		Bottom-hole Conditions		$p_{wf} - p_{tf}$		Difference Between Calculated and Measured Δp (percent)
							Pressure (kg/sq cm abs)	Temperature (°C)	Pressure (kg/sq cm abs)	Temperature (°C)	Measured (kg/sq cm abs)	Calculated (kg/sq cm abs)	
1	8,470	240,000	0.522	10.5	3½	2,900	74.3	27	124.5	74	50.2	33.5	−33.3
2	22,100	85,560	0.557	44	2⅞	1,212	88.8	22.2	100.2	40.1	11.4	14	+22.8
3	29,030	101,000	0.545	8.7	2⅞	2,900	71.3	27	102.9	73.3	31.6	29.2	− 7.6
4	37,500	72,000	0.545	8.7	2⅞	2,900	73.3	27	101.6	73.3	28.4	26.3	− 7.4
5	51,600	92,880	0.557	44	2⅞	1,212	99.2	22.2	113.4	40.1	14.2	14.5	+ 2.1
6	55,500	440,000	0.522	9.9	3½	2,800	88.5	50.3	155.5	87.3	67	40.5	−39.5

Subscripts

b = at reservoir bubble-point conditions
e = external
g = gaseous phase
i = internal
l = liquid phase
M = at the boundary between transition and mist flow regimes
o = oil
S = at the boundary between slug-froth and transition flow regimes
sc = standard conditions (1.033 kg/sq cm abs and 15°C)
tf = wellhead, flowing
w = water
wf = bottom hole, flowing

References

1. Dumitrescu, D. T.: "Strömung an einer Luftblase in senkrechten Rohr," *Zeitung angew. Mathem. Mech.* (1943) **23,** No. 3, 139-149.
2. Moody, L. F.: "Friction Factors in Pipe Flow," *Trans.,* ASME (1944) **66,** 671-684.
3. Davies, R. M., and Taylor, G. I.: "The Mechanics of Large Bubbles Rising Through Extended Liquids and Through Liquids in Tubes," *Proc.,* Royal Society, London (1950) **200A,** 375-390.
4. Poettmann, F. H: "The Calculation of Pressure Drop in the Flow of Natural Gas Through Pipe," *Trans.,* AIME (1951) **192,** 317-326.
5. Poettmann, F. H., and Carpenter, P. G.: "The Multiphase Flow of Gas, Oil and Water Through Vertical Flow Strings," *Drill. and Prod. Prac.,* API (1952) 257-317.
6. Cullender, M. H., and Smith, R. V.: "Practical Solution of Gas-Flow Equations for Wells and Pipelines with Large Temperature Gradients," *Trans.,* AIME (1956) **207,** 281-287.
7. Govier, G. W., Radford, B. A., and Dunn, J. S. C.: "The Upward Vertical Flow of Air-Water Mixtures — I. Effect of Air and Water Rates on Flow Pattern, Holdup and Pressure Drop," *Cdn. J. Chem. Eng.* (Aug. 1957) **35,** 58-70.
8. Govier, G. W., and Short, W. L.: "The Upward Vertical Flow of Air-Water Mixtures — II. Effect of Tubing Diameter on Flow Pattern, Holdup and Pressure Drop," *Cdn. J. Chem. Eng.* (Oct., 1958) **36,** 195-202.
9. Brown, R. A. S., Sullivan, G. A., and Govier, G. W.: "The Upward Vertical Flow of Air-Water Mixtures — III. Effect of Gas Phase Density on Flow Pattern, Holdup and Pressure Drop," *Cdn. J. Chem. Eng.* (April 1960) **38,** 62-66.
10. Griffith, P., and Wallis, G. B.: "Two-Phase Slug Flow," *J. Heat Trans.* (Aug. 1961) **83,** Series C, No. 3, 307-320.
11. Ros, N. C. J.: "Simultaneous Flow of Gas and Liquid as Encountered in Well Tubing," *J. Pet. Tech.* (Oct. 1961) 1037-1049.
12. Hughmark, G. A., and Pressburg, B. S.: "Holdup and Pressure Drop with Gas-Liquid Flow in a Vertical Pipe," *AIChE Jour.* (Dec. 1961) **7,** No. 4, 677-682.
13. Hughmark, G. A.: "Holdup in Gas-Liquid Flow," *Chem. Eng. Prog.* (April 1962) **58,** No. 4, 62-65.
14. Nicklin, D. J., Wilkes, J. O., and Davidson, J. F.: "Two-Phase Flow in Vertical Tubes," *Trans.,* Inst. Chem. Eng. (1962) **40,** 61-68.
15. Duns, H., Jr., and Ros, N. C. J.: "Vertical Flow of Gas and Liquid Mixtures in Wells," *Proc.,* Sixth World World Pet. Cong., Frankfurt (1963) **II,** 451-465.
16. Hagedorn, A. R., and Brown, K. E.: "Experimental Study of Pressure Gradients Occurring During Continuous Two-Phase Flow in Small-Diameter Vertical Conduits," *J. Pet. Tech.* (April 1965) 475-484.
17. Orkiszewski, J.: "Predicting Two-Phase Pressure Drops in Vertical Pipe," *J. Pet. Tech.* (June 1967) 829-838.
18. Aziz, K., Fortems, C. C., and Settari, A.: "Interaction of Wellbore Conditions With Flow in the Reservoir in the Mathematical Simulation of Petroleum Reservoirs," *Proc.,* Eighth World Pet. Cong. (1971) **3,** 209-218.
19. Gilbert, W. E.: "Flowing and Gas-Lift Well Performance," *Drill. and Prod. Prac.,* API (1954) 126-157.
20. Baxendell, P. B.: "Producing Wells on Casing Flow— An Analysis of Flowing Pressure Gradients," *Trans.,* AIME (1958) **213,** 202-206.
21. McAfee, R. V.: "The Evaluation of Vertical-Lift Performance in Producing Wells," *J. Pet. Tech.* (April 1961) 390-398; *Trans.,* AIME, **222.**
22. Baker, W. J., and Keep, K. R.: "The Flow of Oil and Gas Mixtures in Wells and Pipelines: Some Useful Correlations," *J. Inst. Pet.* (May 1961) **47,** No. 449, 162-169.
23. Baxendell, P. B., and Thomas, R.: "The Calculation of Pressure Gradients in High-Rate Flowing Wells," *J. Pet. Tech.* (Oct. 1961) 1023-1028; *Trans.,* AIME, **222.**
24. Tek, M. R.: "Multiphase Flow of Water, Oil and Natural Gas Through Vertical Flow Strings," *J. Pet. Tech.* (Oct. 1961) 1029-1036; *Trans.,* AIME, **222.**
25. Fancher, G. H., Jr., and Brown, K. E.: "Prediction of Pressure Gradients for Multiphase Flow in Tubing," *Soc. Pet. Eng. J.* (March 1963) 59-69; *Trans.,* AIME, **228.**
26. Hagedorn, A. R., and Brown, K. E.: "The Effect of Liquid Viscosity in Two-Phase Vertical Flow," *J. Pet. Tech.* (Feb. 1964) 203-210; *Trans.,* AIME, **231.**
27. Brill, J. P., Doerr, T. C., Hagedorn, A. R., and Brown, K. E.: "Practical Use of Recent Research in Multiphase Vertical and Horizontal Flow," *J. Pet. Tech.* (April 1966) 502-512; *Trans.,* AIME, **237.**
28. Español Herrera, J. H.: "Comparison of Three Methods for Calculating a Pressure Traverse in Vertical Multiphase Flow," MS thesis, U. of Tulsa, Tulsa, Okla. (1968).
29. Tek, M. R., Gould, T. L., and Katz, D. L.: "Steady and Unsteady-State Lifting Performance of Gas Wells Unloading Produced or Accumulated Liquids," paper SPE 2552 presented at SPE-AIME 44th Annual Fall Meeting, Denver, Colo., Sept. 28-Oct. 1, 1969.
30. Español Herrera, J. H., Holmes, C. S., and Brown, K. E.: "A Comparison of Existing Multiphase Flow Methods for the Calculation of Pressure Drop in Vertical Wells," paper SPE 2553 presented at SPE-AIME 44th Annual Fall Meeting, Denver, Colo., Sept. 28-Oct. 1, 1969.
31. Gould, T. L., and Tek, M. R.: "Steady and Unsteady-State Two-Phase Flow Through Vertical Flow Strings," paper SPE 2804 presented at SPE-AIME Second Symposium on Numerical Simulation of Reservoir Performance, Dallas, Feb. 5-6, 1970.
32. Harmathy, T. Z.: "Velocity of Large Drops and Bubbles in Media of Infinite or Restricted Extent," *AIChE Jour.* (June 1960) **6,** No. 2, 281-288.
33. Zuber, N., Staub, F. W., Bijwaard, G., and Kroeger, P. G.: "Steady State and Transient Void Fraction in Two-Phase Flow Systems," *Report* EURAEC-GEAP No. 5417, **1,** General Electric Co., San Jose, Calif. (Jan. 1967).
34. Standing, M. B., and Katz, D. L.: "Density of Natural Gases", *Trans.* AIME (1942) **146,** 140-149.
35. Sarem, A. M.: "Z-Factor Equation Developed for Use in Digital Computers," *Oil and Gas J.* (Sept. 18, 1961) **59,** No. 38, 118.
36. Carlile, R. E., and Gillett, B. E.: "Computer Programming and Mathematical Techniques for Engineers — 74," *Oil and Gas J.* (July 19, 1971) **69,** No. 29, 68-72.
37. Lee, A. L., Gonzales, M. H., and Eakin, B. E.: "The Viscosity of Natural Gases," *J. Pet. Tech.* (Aug. 1966) 997-1000; *Trans.,* AIME, **237.**
38. Long, G., and Chierici, G. L.: "Salt Content Changes Compressibility of Reservoir Brines," *Pet. Eng.* (July 1961) **33,** No. 7, B-25 through B-31.
39. "How Temperature Affects Viscosity of Salt Water," *World Oil* (Aug. 1, 1967) **165,** No. 2, 68.
40. Katz, D. L., Monroe, R. R., and Trainer, R. P.: "Surface Tension of Crude Oils Containing Dissolved Gases," *Pet. Tech.* (Sept. 1943) *TP 1624.*
41. Standing, M. B.: "A Pressure-Volume-Temperature Correlation for Mixtures of California Oils and Gases," *Drill. and Prod. Prac.,* API (1947) 275-287.

42. Standing, M. B., and Katz, D. L.: "Density of Crude Oils Saturated with Natural Gas," *Trans.*, AIME (1942) **146**, 159-165.
43. Lasater, J. A.: "Bubble-Point Pressure Correlation," *Trans.*, AIME (1958) **213**, 379-381.
44. Frick, T. C.: *Petroleum Production Handbook*, Society of Petroleum Engineers of AIME, Dallas (1962) **2.**
45. Chew, J. N., and Connally, C. A., Jr. "A Viscosity Correlation for Gas-Saturated Crude Oils," *Trans.*, AIME (1959) **216**, 23-25.
46. Braden, W. B.: "A Viscosity-Temperature Correlation at Atmospheric Pressure for Gas-Free Oils," *J. Pet. Tech.* (Nov. 1966) 1487-1490; *Trans.*, AIME **237.**
47. Beal, C.: "The Viscosity of Air, Water, Natural Gas, Crude Oil and Its Associated Gases at Oil Field Temperatures and Pressures," *Trans.*, AIME (1946) **165**, 94-115.
48. Calhoun, J. C., Jr.: *Fundamentals of Reservoir Engineering*, U. of Oklahoma Press, Norman, Okla. (1953).

Paper (SPE 4316) was first presented at the SPE-AIME European Spring Meeting, held in London, May 2-3, 1973. © Copyright 1974 American Institute of Mining, Metallurgical, and Petroleum Engineers, Inc.
This paper will be printed in *Transactions* volume 257, which will cover 1974.

Discussion

M. R. Tek, SPE-AIME, U. of Michigan

The paper by Chierici and his associates is timely, relevant, and interesting. The authors are to be congratulated for their contribution to our understanding and analysis of pressure gradients in slug flow and for adding meticulously calculated and organized two-phase flow data to existing banks on the subject. Their data have already proved valuable in more precise determination of flow regime boundaries, as shown by Gould *et al.*[1] in a companion paper.

The use of locally prevailing flow regime determination in pressure-drop calculations through the use of selective correlations has been confirmed by the authors. The procedure, first credited to Orkiszewski and also confirmed by Gould *et al.*, appears to be well on the way to becoming an industry standard as it keeps being improved by successive papers.

Although the statistical significance of average error and standard deviation must be interpreted with caution because of the small sample size, the new method proposed for calculating density gradients in slug flow regime appears to be an improvement over Orkiszewski's method, which requires an empirical liquid distribution coefficient. Chierici *et al.'s* use of $v_s = 24$ cm/sec — an apparently universal terminal slip velocity for bubble flow — may be subject to question because it ignores the effect of system physical properties on terminal velocity of ascent. If more sophistication is desired or justified, the readers are directed to study the works of Harmathy,[2] Levich,[3] and Wallis[4] in this area.

The relative difficulty the authors have encountered in predicting as well the performance of gas wells subject to water production is believed to be due largely to the approximate location of slug-transition-annular mist flow regime boundaries as recently revised by Gould *et al.*[1]

References

1. Gould, T. L., Tek, M. R., and Katz, D. L.: "Two-Phase Flow Through Vertical, Inclined, or Curved Pipe," *J. Pet. Tech.* (Aug. 1974) 915-926; *Trans.*, AIME, **257.**
2. Harmathy, T. B.: "Velocity of Large Drops and Bubbles in Media of Infinite or Restricted Extent," *AIChE Jour.* (June 1960) **6**, No. 2, 281-288.
3. Levich, G. G.: *Physico Chemical Hydrodynamics*, Prentice-Hall, Inc., Englewood Cliffs, N. J. (1962).
4. Wallis, G. B.: "One-Dimensional Two-Phase Flow," McGraw-Hill Book Co., Inc., New York (1969).

Discussion

J. Orkiszewski, SPE-AIME, Esso Australia Ltd.

I have only two points to make in my discussion:

1. I disagree with the authors in their derivation of Eq. 15 from Eqs. 13 and 14, and
2. From experience, I find the number of data that the authors have presented to be inadequate to ascertain the universality of their method.

Chierici *et al.* erred in assuming that the correlative equations derived by Griffith and Wallis for laminar/transition flow (Eq. 13) and by Nicklin *et al.* for turbulent flow (Eq. 14) are interrelated. In my work, the bubble-rise velocity was interpreted to be a function of the turbulent or laminar nature of liquid flow; this means that Eqs. 13 and 14 are not directly related. The following is support for my position.

1. When the curves in the transition range in Fig. 3 of the Chierici *et al.* paper are compared with those in Fig. 9 of the original Griffith and Wallis paper, all the former curves, other than the "laminar line" ($N_{Re} = 3{,}000$ or less), have curvatures reversed from those originally presented by Griffith and Wallis.

2. The value of C_2 presented in Fig. 3 tends to extrapolate to infinity. This is contrary to the original postulations of Griffith and Wallis, as shown in the following excerpt from their original work:

> The plots that gave best results are shown in Fig. 9. Points were found to fall in the "laminar line" to a good degree of accuracy for bubble Reynolds numbers below 3,000. For the bubble Reynolds number between 3,000 and 5,000 results do not

coordinate well and are scattered around in the general area of the graph, presumably a transition region where turbulent flow is starting to be initiated. At higher bubble Reynolds numbers, results are again more consistent but with the present apparatus it was impossible to explore the full developed turbulent region properly. It seems logical though that as the velocity profile becomes flatter at large pipe Reynolds number C_2 should approach one. This appears to be the case.

3. The lowest line in Fig. 3, marked with a bubble Reynolds number of 8,000 and attributed to me, was determined by me by direct calculation of C_2 using the Nicklin *et al.* approach, which is the author's Eq. 14. Note the marked divergence between the line based on the actual work of Nicklin *et al.* and the line extrapolated by the authors for the turbulent range. I had assumed the lower line to be a limited "turbulent line" much like that which Griffith and Wallis set out as their "laminar line." The lower Reynolds numbers were extrapolated simply using the same slope as the "turbulent line." This is not correct, as one would expect these curves to merge eventually with the "turbulent line."

My initial effort in using the Griffith and Wallis method provided calculated results in excellent agreement with measured values of 17 wells in much the same degree as reported by Chierici *et al.* Additional computations, however, indicated that the Griffith and Wallis method was not universally applicable; hence the development of my liquid distribution coefficient. You will note that the coefficient is used in conjunction with the liquid fraction, which is a partial reply to the question posed by Chierici *et al.* as to its meaning; but its only true meaning is that it relates theory to reality.

Authors' Reply to Tek and Orkiszewski

We appreciate receiving the Discussions by Tek and Orkiszewski. The points they raise are very important.

As Tek recalled, there are several correlations for evaluating v_s in the bubble regime; some of them have been quoted in our paper. The use of $v_s = 24$ cm/sec, as suggested by Griffith and Wallis (Ref. 10 of our paper), gave us a satisfactory match of the experimental pressure-drop values. That is why we have not resorted to more sophisticated methods to compute v_s.

We agree with Tek that a low N_{lv} values the standard flow regime map might not be reliable; the contribution by Gould *et al.* (Ref. 1 of Tek's Discussion) in this area is to be commended.

We have always been aware that the number of cases presented is not large enough to ascertain the universality of our method. The cases considered have been intentionally limited to those where reliable PVT data were available.

If we have correctly grasped Orkiszewski's point about "non interrelation" between the equations for v_b of Griffith and Wallis and those of Nicklin *et al.* (Ref. 14 of our paper), the following explains our point of view.

The Griffith and Wallis data cover the $(N_{Re})t$ range up to 6,000. The Nicklin *et al.* data go above this limit; their equation (Eq. 14 of our paper) with $\Lambda = 0.2$ permits evaluating v_b in the $(N_{Re})t > 8{,}000$ range.

Eq. 14 can be made to fit the Griffith and Wallis curves for C_2, once the proper $\Lambda[(N_{Re})_b, (N_{Re})_t]$ function is calculated. This function is presented in Fig. R-1. The following points deserve consideration:

1. At high $(N_{Re})_t$ values all Λ curves converge towards $\Lambda = 0.2 =$ constant, this value being given by Nicklin *et al.* for turbulent flow.

2. For $(N_{Re})_b > 8{,}000$, Λ is constant at 0.2, irrespective of $(N_{Re})_t$. This substantiates the continuity between the Griffith and Wallis and the Nicklin *et al.* results.

Obviously, the Griffith and Wallis equation for v_b (Eq. 13 of our paper) can be extended to cover the entire range of $(N_{Re})_t$. To this end, C_2 values are calculated for $(N_{Re})_t > 6{,}000$ from Eq. 15 and Λ as given in Fig. R-1, preventing $(N_{Re})_b$ from going below 3,000. C_2 curves presented in Fig. 3 of our paper have been calculated this way.

Consequently, to calculate v_b in the slug-froth flow regime it is immaterial whether one uses Eq. 13 with C_2 values given in Fig. 3 or Eq. 14 with Λ values given in Fig. R-1.

From Eq. 15 and Fig. R-1 it is apparent that C_2 approaches 1.00 for increasing values of $(N_{Re})_b$. In our interpretation, this is the meaning of Griffith and Wallis' statement "at large pipe Reynolds number, C_2 should approach 1," this statement being confirmed by the trend shown in Fig. 9 of their paper. **JPT**

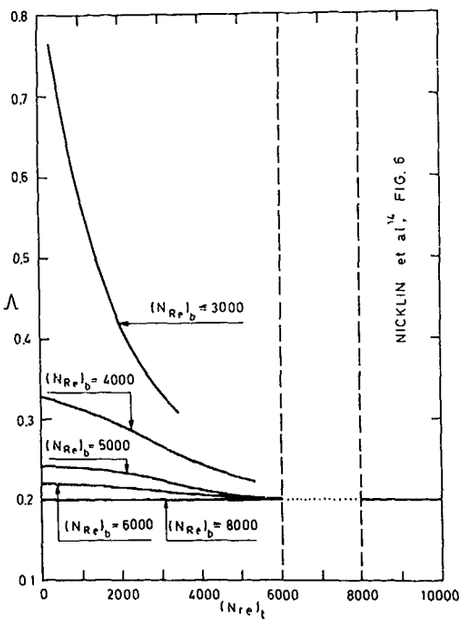

Fig. R-1—(N_{Re}) t vs Λ, calculated from Griffith and Wallis' Fig. 9.